ARTICLE OPEN

Check for updates

Optogenetic stimulation of midbrain dopaminergic neurons rescues hippocampal synaptic plasticity deficits in a mouse model of Alzheimer's disease

Serena Ficchì[1], Emma Cauzzi[1], Livia La Barbera[1,2], Maria Luisa De Paolis[1,2], Gilda Loffredo[1], Elena Spoleti[1], Irene Ferrari[1], Luana Saba[1,2], Filippo Biamonte[3], Annalisa Nobili[1,2], Paraskevi Krashia[2,4,5] and Marcello D'Amelio[1,2,5]✉

We previously demonstrated that the Tg2576 mouse model of Alzheimer's Disease (AD) exhibits degeneration of midbrain dopaminergic neurons, resulting in reduced dopamine (DA) outflow in the hippocampus. These impairments temporally coincide with synaptic plasticity deficits at CA3-CA1 synapses. Notably, systemic administration of dopaminergic agents/drugs rescues the hippocampal deficits in Tg2576 mice. However, whether direct stimulation of the remaining midbrain dopaminergic neurons can restore glutamatergic transmission and rescue plasticity dysfunctions in the context of AD remains unexplored. Here, using both 6-hydroxydopamine (6-OHDA) neurotoxic lesion and optogenetic stimulation in C57BL/6N and DATCre/Tg2576 mice, respectively, we demonstrate that midbrain DA is essential for hippocampal High-Frequency Stimulation-induced Long-Term Potentiation (HFS-LTP) in CA3-CA1 synapses. Indeed, lesioning midbrain DA neurons with 6-OHDA abolishes HFS-LTP and impairs novel object recognition memory. Conversely, optogenetic activation of the midbrain-hippocampal dopaminergic pathway in DATCre/Tg2576 mice enhances glutamatergic transmission and rescues plasticity deficits. Our results highlight the phase-specific role of DA in HFS-LTP, since 6-OHDA lesion affects the late but not the early phase, aligning with prior studies on D1/D5 receptor involvement in protein synthesis-dependent plasticity. Furthermore, we provide novel insights into midbrain DA neuron regulation, demonstrating that phasic, but not prolonged, optogenetic stimulation effectively engages DA neuron activity, restoring hippocampal function in Tg2576 mice. Notably, phasic DA release induces "DA-LTP" *via* D1/D5 receptors, and restores HFS-LTP in CA3-CA1 synapses of AD mice, underscoring a potential compensatory mechanism counteracting plasticity deficits induced by DA neuron degeneration in Tg2576 mice. These findings support targeting the dopaminergic midbrain as a promising strategy for AD treatment, complementing pharmacological and non-invasive neuromodulatory approaches.

Translational Psychiatry (2025)15:371 ; https://doi.org/10.1038/s41398-025-03588-w

INTRODUCTION

It is well established that the dopaminergic neurotransmission from the midbrain is fundamental for motivation and reward *via* its projections to mesolimbic targets like the Nucleus Accumbens and Striatum [1]. Additionally, dopamine (DA) released from the midbrain is implicated in memory and learning processes *via* projections from the Ventral Tegmental Area and Substantia Nigra *pars compacta* (VTA/SNpc) to the dorsal hippocampus [2–6]. Indeed, the midbrain was long thought to be the sole source of DA in the dorsal hippocampus. Yet, recent studies have challenged this conventional view by suggesting that the *Locus Coeruleus* (LC) represents the predominant source of dopaminergic input to this brain area [7–9]. Building on these findings, a refined view on the roles of the midbrain dopaminergic innervation of the hippocampus has emerged, in which VTA/SNpc-derived DA is primarily involved in reinforcement learning, in formation of contextual or aversive learning and in modulating reward-related memory functions [2–6]. These works collectively underscore the crucial role of midbrain DA in regulating hippocampal activity under distinct *physiological* conditions.

Despite these insights, a critical question remains unanswered: is the enhancement of the DA signalling from the VTA/SNpc sufficient to rescue hippocampal function under *pathological* conditions marked by VTA degeneration? In this regard, our recent findings indicate that the VTA DA neurons progressively degenerate in the Tg2576 mouse model of Alzheimer's Disease (AD), and that this neuronal loss is concomitant with impairments in hippocampal neuron function, deficits in Long-Term Potentiation (LTP) at CA3-CA1 synapses of the dorsal hippocampus and in memory defects [10–16]. Systemic pharmacological interventions, including L-DOPA and monoamine oxidase inhibitors (e.g., selegiline), can fully restore LTP deficits and improve hippocampus-

[1]Department of Medicine and Surgery, Università Campus Bio-Medico di Roma, Via Alvaro del Portillo, 21, 00128 Rome, Italy. [2]Department of Experimental Neurosciences, IRCCS Santa Lucia Foundation, Via del Fosso di Fiorano, 64, 00143 Rome, Italy. [3]CeMAD Translational Research Laboratories, Department of Medical and Surgical Sciences, Fondazione Policlinico Universitario "A. Gemelli" IRCCS, Largo Agostino Gemelli, 8, 00168 Rome, Italy. [4]Department of Sciences and Technologies for Sustainable Development and One Health, Università Campus Bio-Medico di Roma, Via Alvaro del Portillo, 21, 00128 Rome, Italy. [5]These authors contributed equally: Paraskevi Krashia, Marcello D'Amelio. ✉email: m.damelio@unicampus.it

Received: 25 March 2025 Revised: 31 July 2025 Accepted: 28 August 2025
Published online: 06 October 2025

dependent memory performance in Tg2576 mice and other AD mouse models [14, 15, 17–21]. Yet, these treatments primarily act at the postsynaptic level. Whether direct activation of the presynaptic VTA/SNpc dopaminergic fibres during the ongoing neurodegeneration can effectively rescue hippocampal LTP remains an open question. This is particularly pressing given the already sparse dopaminergic innervation of the dorsal hippocampus from the midbrain [5–7, 22].

To address this, we first aimed to confirm the necessity of midbrain-derived DA for dorsal hippocampal LTP. Thus, in the first part of our study we used direct infusion of 6-hydroxydopamine (6-OHDA) into the VTA/SNpc to selectively lesion dopaminergic neurons and assess the consequent effects on CA3-CA1 synaptic plasticity and novel object recognition (NOR) memory. Subsequently, in the second part, we employed optogenetic stimulation of VTA/SNpc dopaminergic projections in the dorsal hippocampus of Tg2576 mice at an advanced stage of midbrain DA neuron degeneration to determine whether this experimental approach is sufficient to potentiate the glutamatergic neurotransmission and restore LTP deficits.

This study elucidates the critical role of midbrain-derived DA in regulating hippocampal synaptic plasticity, establishing a mechanistic foundation for the development of targeted therapeutic strategies to mitigate deficits associated with dopaminergic neurodegeneration. Such therapies, if proven effective in activating the VTA dopaminergic neurons, could hold promise against cognitive decline and neuropsychiatric symptoms associated with DA loss, including anxiety and apathy, which often characterise the early stages of the disease [23]. Beyond its implications for AD, our findings also extend to non-motor symptoms of Parkinson's Disease, where disruptions in mesocorticolimbic DA transmission contribute to cognitive decline, affective disturbances and impaired hippocampal-dependent memory, symptoms that may be ameliorated following mesocorticolimbic stimulation. By refining our understanding of the dopaminergic modulation of hippocampal circuits, this work paves the way for innovative interventions aimed at restoring synaptic integrity and cognitive function in neurodegenerative disorders.

METHODS

Animals

C57BL/6N mice (Charles River, Italy) were used at 2–3 months of age. Heterozygous DATCre^{IRES} female mice (The Jackson Laboratory, Strain #006660) were crossed with heterozygous Tg2576 males (Taconic, APPSWE - Model #1349) to generate DATCre/WT and DATCre/Tg2576 mice that were used at 5–6 months of age. Animals were housed with *ad libitum* food and water (12 h light/dark cycle). For electrophysiological experiments we used both male and female mice; for all other experiments only male mice were used. Experiments complied with the ARRIVE guidelines and were carried out according to ethical guidelines of the European Council (2010/63/EU). Authorization was approved by the Italian Health Ministry.

Stereotaxic injections

Mice were anaesthetized with Rompun (20 mg/mL, 0.5 mL/kg; Bayer) and Zoletil (100 mg/mL, 0.5 mL/kg; Virbac; intraperitoneally, i.p.) and positioned in a stereotaxic apparatus.

C57BL/6N mice were injected in the left midbrain with 6-OHDA (Sigma-Aldrich) prepared at 7.6 mg/mL (calculated as free-base), dissolved in 0.2 mg/mL ascorbic-acid (Tocris) prepared in 0.9% sterile saline, and continuously kept on ice. Each mouse was injected with 2.5 µg in 0.4 µL (flow-rate 40 nL/min). Thirty minutes before stereotaxic injection, mice received 10 mL/kg (2.85 mg/mL as free base, i.p.) of desipramine-hydrochloride (Sigma-Aldrich), a norepinephrine (NE) reuptake-inhibitor, to prevent midbrain-projecting NE fibre degeneration. Control mice were injected with 0.9% sterile saline solution (Saline mice). C57BL/6N mice were injected at 2 months of age and analysed one-month post-lesion. The accuracy of the injection was controlled by counting of Tyrosine Hydroxylase-positive (TH$^+$) cells in the midbrain; mice without lesion were excluded.

For optogenetic stimulation, DATCre/WT and DATCre/Tg2576 mice were injected in the midbrain with the adeno-associated virus (AAV) expressing the Cre-dependent Channelrhodopsin2-eYFP fusion protein (AAV-EF1a-DIO-hChR2(H134R)-eYFP, gift from Karl Deisseroth (UNC Vector Core). Mice were injected bilaterally with 1 µL/hemisphere of AAV (flux 80 nL/min) at 5 months of age and used 30 days later, to ensure viral expression. Control mice underwent the same surgery procedure with the same AAV, but during experiments we did not apply the optogenetic stimulation (Sham mice). The accuracy of midbrain injection was controlled by eYFP signal; the results obtained from mice showing misplaced injection were discarded.

Overall, midbrain injections were performed in the VTA (AP: −3.2, ML: ±0.35, DV: −4.4) [24]. For infusions we used 1 µL Hamilton syringes (Neuros7001 model) mounted on a Harvard Apparatus Pump-11 Elite-Nanomite.

Immunofluorescence

Mice were anaesthetized with Rompun/Zoletil and perfused transcardially with phosphate buffer (PB; 0.1 M, pH 7.4) followed by 4% paraformaldehyde in PB. Brains were postfixed in 4% paraformaldehyde overnight (4 °C) and immersed in 30% sucrose solution (4 °C) until sinking. Coronal sections (thickness = 30 µm) were obtained using a cryostat and collected in 0.02% PB-Sodium Azide. Analysis of 6-OHDA or Saline mice was performed in the hemisphere ipsilateral to the lesion.

Slices from 6-OHDA/Saline and DATCre mice containing the midbrain or LC were incubated with mouse anti-TH antibody in PB containing 0.3% Triton X-100 (PB-TX 0.3%) overnight at 4 °C.

For hippocampal TH and NET fibres, sections were incubated in citrate buffer (10 mM Sodium citrate, pH 6.0, containing 0.05% Triton X-100; 20 min, 75 °C), rinsed in PB, immersed in blocking solution (5% donkey serum, 0.2% Triton X-100 in PB; 1 h, RT) and incubated with primary antibody in the same solution (overnight at 4 °C) [12].

For Aβ staining, sections were pretreated with M.O.M. (1:1000; 2 h, at RT) diluted in permeabilization solution (PB with 0.3% Triton X-100), and incubated with primary antibodies overnight at 4 °C in permeabilization solution.

To confirm the midbrain expression of AAV-EF1a-DIO-hChR2(H134R)-eYFP in DATCre/WT and DATCre/Tg2576 mice, slices used for electrophysiological recordings were fixed in 4% paraformaldehyde overnight, washed three times in PB, immersed in PB-Sodium Azide 0.02% and then visualised under a confocal microscope for eYFP expression.

After primary antibodies and washes with PB, sections were incubated with secondary antibodies in the same solution of primary antibody (2 h, RT), then counterstained with NeuroTrace 435/455 or DAPI (1:1000, Serva), and mounted with anti-fade medium (Fluoromount, Sigma Aldrich).

Slices were examined using a Nikon Eclipse-Ti2 confocal microscope. The specificity of the immunofluorescence labelling was confirmed by omission of primary antibodies and use of normal serum instead (negative controls). All images were exported in TIFF.

For fibre density analysis, images were acquired with a 20x-objective by Z-stacks, then processed by maximum-intensity projection. Samples were captured with identical Z-stack thickness and laser settings. 3D-images were collected from at least 4–5 slices processed simultaneously. The fibre density was quantified manually from the different hippocampal subfields (CA1, CA3, Dentate Gyrus; DG) and was expressed as number of fibres/250 µm [12]. Fibre density for the total hippocampus was obtained by averaging the density of each subfield per animal.

Primary antibodies: TH (1:1000, Millipore; MAB318; RRID: AB_2201528 and 1:1000, Abcam; #AB112; RRID: AB_297840); NET (1:500; Atlas Antibodies #AMAb91116; RRID: AB_2665806); hAPP695 (6E10; 1:500, BioLegend #803001; RRID: AB_2564653).

Secondary antibodies: Alexa Fluor-488 donkey anti-mouse (1:200; #R37114; RRID: AB_2556542), Alexa Fluor-488 donkey anti-rabbit (1:200; #A-21206; RRID: AB_2535792), NeuroTrace 435/455 Blue Fluorescent Nissl Stain (1:200, #N21479), NeuroTrace 640/660 Deep-Red Fluorescent Nissl Stain (1:200, #N21483; RRID: AB_2572212).

Exclusively for the representative confocal images, after the quantitative analysis, LUTs were equally increased at the same level for all groups of a given experiment. Quantitative analysis was performed on raw images.

Stereological cell counting

Sections processed for immunofluorescence were used for counting the number of TH$^+$ neurons in the VTA, SNpc (every second slice) and LC (every third slice) of 6-OHDA/Saline mice ipsilateral to the lesion, or in the total

VTA and unilateral SNpc in DATCre mice. The area boundaries were delineated by TH staining, in accordance to Paxinos guidelines [24]. We applied an optical fractionator stereological design using the Stereo Investigator System (2023 v, MicroBrightField). A stack of MAC5000 controller modules (Ludl Electronic Products, Ltd) was interfaced with a Zeiss Microscope (Axio Imager KMAT) with a motorized stage and a Zeiss Axiocam 506-mono with a working high-end computer. We applied a 3D optical fractionator counting probe (*x*, *y*, *z* dimension of 50 × 50 × 25 µm). The brain areas were outlined using the 5x objective; neurons were marked with a 100x-oil-immersion (VTA and SNpc) or a 40x-objective (LC).

The total TH^+ neuron number was estimated according to Equation 1:

$$N = SQ \times (1/ssf) \times (1/asf) \times (1/tsf)$$

where SQ represents the number of neurons counted in all optically sampled fields of the area of interest, ssf is the section sampling fraction, asf is the area sampling fraction and tsf is the thickness sampling fraction.

High performance liquid chromatography (HPLC)

Hippocampal catecholamines (DA and NE) and their metabolites (DOPAC and HVA for DA; MOPEG for NE) were quantified using an HPLC system (UltiMate® 3000, ThermoFisher) coupled with a Coulochem electrochemical detector (6011RS Ultra Coulometric Analytical Cell, ThermoFisher). Following cervical dislocation and decapitation, the left hippocampus of 6-OHDA or Saline mice was dissected on ice and stored at −80 °C until analysis. On the day of analysis, frozen samples were homogenized on ice with a 4:1 mix of 0.05 M $HClO_4$ and antioxidant solution (containing, in mM: Na_2-EDTA 0.27, acetic acid 100, ascorbic acid 0.0125). The homogenate was lysed mechanically, sonicated on ice and centrifuged at 10.000 rpm (20 min, 4 °C). The supernatant was transferred to a new tube and the pellet was weighed. For each sample, 20 µL were injected into the HPLC-ECD system (runtime: 60 min; flow-rate: 0.6 mL/min). Standards were prepared fresh using the same solutions and quantities as for tissue samples. The chromatographic separation was performed using a Hypersil GOLD aQ-C18 column (150 × 3 mm, 5 µm) kept at 37 °C and fitted with an aQ-C18 drop-in guard pre-column (10 × 3 mm, 5 µm). The mobile phase consisted of 5% methanol and buffer solution (0.1 M Na-Phosphate, 0.1 mM Titriplex® III and 0.5 µM 1-Octanesulfonic-Acid Na-salt, pH 3.6 adjusted with 85% Ortho-Phosphoric-acid), filtered through a 0.22 µm cellulose-ester membrane. We applied a potential of +450 mV to the dual-inline flow-through micro-porous graphitic carbon-working electrodes, with 1 nA-gain for ECRS1 and 10 nA-gain for ECRS2. The chromatograms were processed using Chromeleon™ Software (v7.0 ThermoFisher). The concentration of metabolites in the samples was determined based on the corresponding peak heights and then normalized to the pellet weight.

Brain slicing

After mouse dislocation, the brain quickly removed and parasagittal slices containing the dorsal hippocampus [10], or horizontal slices containing the midbrain [25], were cut with a Leica VT1200S vibratome (thickness: 300 µm) in ice-cold oxygenated (95% O_2, 5% CO_2) sucrose-based solution (in mM: KCl 3, NaH_2PO_4 1.25, $NaHCO_3$ 26, $MgSO_4$ 10, $CaCl_2$ 0.5, glucose 25, sucrose 185; ~300 mOsm, pH 7.4). Brain slices were incubated for 40 min in oxygenated artificial Cerebro-Spinal Fluid (aCSF, containing, in mM: 124 NaCl, 1.25 NaH_2PO_4-H_2O, 26 $NaHCO_3$, 3 KCl, 10 glucose, 1 $MgSO_4$, 2 $CaCl_2$, pH 7.3–7.4) at 32 °C and then transferred at room temperature in aCSF for at least 30 min before recordings.

Optogenetic stimulation

Ex-vivo optogenetic stimulation was achieved *via* delivery of blue-green light (λ: ~527 nm) using the laser source by a Lambda421 (Sutter Instruments) beam combiner, controlled by the MetaFluor software via pClamp11 (Molecular Devices). Phasic and prolonged light stimulation was used to excite ChR2-expressing dopaminergic neurons in the VTA. Dopaminergic fibres in the hippocampus were stimulated by the same phasic protocol applied to the VTA. The phasic protocol consisted of a train of three 5 ms-long light square pulses, each separated by 15 ms (intra-burst frequency 66.66 Hz). The total duration was 1 s long (inter-burst frequency 1 Hz) and was delivered 25 times [26]. For prolonged light stimulation a single 800 ms-long light pulse was delivered.

Electrophysiology

A brain slice was placed under an upright microscope (BX51WI Olympus) and continuously perfused with oxygenated aCSF (29–30 °C; 3–4 mL/min). Recordings were performed using a MultiClamp-700B Amplifier, digitized with Digidata-1550B and computer-saved with pClamp11 (Molecular Devices). Pipettes (2-3 MΩ) were pulled from borosilicate thin-wall filamented capillaries (TW150F-4, World Precision Instruments).

Extracellular recordings: VTA. Acute horizontal midbrain slices were used to record spontaneously active dopaminergic neurons in the lateral VTA [27]. DA neurons were visually identified by the eYFP fluorescence. The accurate position of the recorded cells in the lateral VTA was assessed by checking the position of the electrode under a 4x objective at the end of each experiment.

Single unit activity was recorded with aCSF-filled glass pipettes by moving the electrode towards the neuron surface until firing was detected. Traces were recorded using the amplifier's I = 0 mode, filtered on-line with high-pass (1 Hz) and low-pass filtering (0.5 kHz) and digitized at 20 kHz. Once firing was detected, baseline activity was recorded for at least 3 min, after which the optogenetic protocols (phasic and prolonged) were applied. Between protocols, the neuron's baseline activity was recorded to monitor cell activity.

Field excitatory postsynaptic potentials (fEPSPs): dorsal hippocampus. For recording of CA3-to-CA1 fEPSPs in parasagittal hippocampal slices, the recording and stimulating electrodes were placed in the *stratum radiatum* at a ~ 300 µm distance apart. Electrodes were filled with aCSF. fEPSPs were evoked by Schaffer collateral stimulation (100 µs square pulses), acquired at 20 kHz and filtered off-line with a 10 kHz low-pass Bessel. Input-output curves of fEPSP slopes were obtained at 10 µA steps of increasing stimulation every 30 s.

For ex-vivo pharmacological treatment, the D1/D5 receptor antagonist SCH-23390 (20 µM, purchased from Selleck Chemicals) was added to the aCSF solution *via* bath perfusion. Photostimulation was applied after at least 10 min of stable fEPSP responses in the presence of the antagonist, to ensure that a steady-state level of D1/D5 receptor antagonism was reached.

For LTP, after at least 10 min of baseline responses at half-maximal intensity to assess fEPSP slope stability, the slice was challenged by two pulse trains at 100 Hz (1 s duration each, 20 s interval) followed by test stimulation for at least 1 h. The LTP magnitude was evaluated as the fEPSP mean slope during the final 5 min, normalized to the mean slope of the final 5 min during baseline.

To test the effect of the optogenetic stimulation on fEPSP slope in DATCre mice, stable fEPSP responses were recorded for at least 10 min at half-maximal stimulation, before applying the phasic light stimulation protocol immediately prior to the high-frequency train of electric stimulation.

Open field and novel object recognition (NOR) tests

Behavioural testing was conducted in a dimly-lit (25 lux) open field plexiglass arena (60 × 60 × 30 cm), consisting of dark-grey walls and a white floor. On Day1 (D1), each mouse was placed in the centre of the arena and allowed to freely-explore for 10 min, during which movements were recorded. We analysed the total distance travelled (in cm) and time spent (in s) in the centre and periphery of the arena.

The NOR test followed, comprising three phases: habituation, training and testing. During habituation (D1), mice were familiarized with the empty arena for 10 min. On the following day (D2), during the training phase, mice were exposed for 10 min to two identical objects (yellow wooden spheres) placed in the centre of the arena, equidistant from the arena centre and walls. Afterward, mice were returned to their home cages. On Day 3 (D3), mice were reintroduced into the arena for 10 min to perform the test phase. One of the objects was replaced with a novel, unfamiliar object (a light-grey wooden cone). During both the training and testing phases, mice were left to freely-explore the objects, and the exploration time was recorded. The latter (in s) was defined as the time touching or climbing on an object or sniffing it at a distance of at least 2 cm. Object placement was randomized and counterbalanced across experimental groups. To minimize olfactory cues between sessions or mice, both the arena and objects were cleaned with 5% ethanol after each session.

Power analysis, randomization, blinding

We performed power analysis using the G*Power software (3.1.9.7 v) to determine the sample numbers for the experimental groups. Input parameters were: power of 0.8; errors of 0.05; standard deviations were

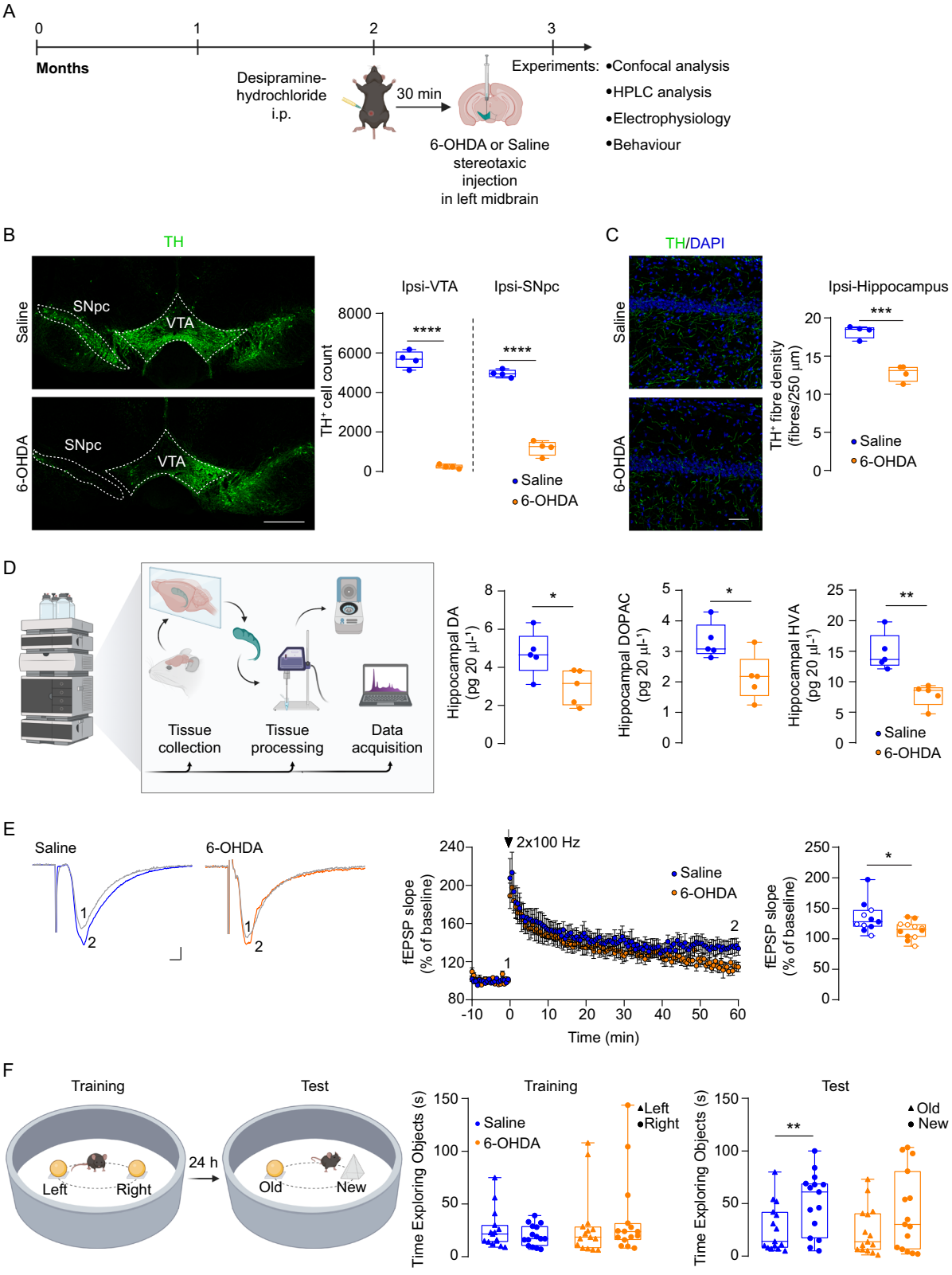

obtained from previous publications where similar experiments were performed on naïve Tg2576 mice [10, 12, 13]. The experimental units are specifically described in each figure legend.

Animal randomization (i.e. how mice born from the same litter were 'destined' for each experimental group) was performed with a random number table, matched by sex.

All researchers were blinded to the genotype/treatment; un-blinding occurred after analysis.

Statistical analysis

Analyses were performed using Prism8.01 (GraphPad). Data were checked for normality using the Shapiro-Wilk and D'Agostino-Pearson tests. Data

Fig. 1 Midbrain 6-OHDA causes loss of DA in the dorsal hippocampus, inducing LTP and behavioural deficits in 3-month-old mice. A 2-month-old C57BL/6N mice were unilaterally infused in the midbrain with 6-OHDA or Saline. 30 min before stereotaxic injection, mice received an i.p injection of the NE reuptake inhibitor desipramine. Mice were used for experimental sessions 1 month after the midbrain lesion. **B** Representative coronal sections of the midbrain, showing immunofluorescence for TH^+ neurons in Saline and 6-OHDA 3-month-old mice (scale bar: 500 µm), and stereological TH^+ cell count in the ipsilateral VTA (n = 4 mice / group. Welch's *t*-test: ****p < 0.0001) and SNpc (n = 4 mice / group. Unpaired *t*-test: ****p < 0.0001). **C** Confocal images and plots showing TH^+ fibre density in the ipsilateral dorsal hippocampal (expressed as fibres / 250 µm; scale bar: 50 µm) in 3-month-old Saline and 6-OHDA mice (n = 4 mice / group. Unpaired *t*-test: ***p = 0.0002). Nuclei are counterstained with DAPI. **D** Schematic representation of the experimental procedure for HPLC analysis of total hippocampal levels of DA, NE and relative metabolites in the ipsilateral hippocampus from 3-month-old Saline and 6-OHDA mice. The plots show tissue levels of DA, DOPAC and HVA, expressed as pg in 20 µL of supernatant (n = 5 mice / group. DA: Unpaired *t*-test: *p = 0.0294; DOPAC: Unpaired *t*-test: *p = 0.0242; HVA: Unpaired *t*-test: **p = 0.0022). **E** Representative traces showing fEPSPs elicited in the dorsal hippocampus at half maximal Schaffer collateral stimulation in acute slices from 3-month-old Saline and 6-OHDA mice during baseline (1) and 1 h (2) after two HFS trains (scale bar: 2 ms; 0.2 mV). The plots on the right show the time-course of normalized, average fEPSP slope (± s.e.m.) and the pooled data (Saline: n = 11 slices / 3 mice; 6-OHDA: n = 12 slices / 4 mice. Unpaired *t*-test: *p = 0.0243). The vertical arrow indicates the timing of the HFS protocol. Empty dots refer to female mice, while full dots to males. **F** Graphical representation of the training and test (24 h later) phases of the NOR test performed for 3-month-old Saline and 6-OHDA mice, and plots showing the exploration time spent with the left/right and old/new object during the training and test, respectively (n = 15 mice / group; for Saline, Paired *t*-test: **p = 0.0025). [Schematics were created using BioRender (https://biorender.com)].

from two groups (i.e. Saline vs 6-OHDA or DATCre/WT vs DATCre/Tg2576) were analysed with 2-tailed parametric unpaired (*t*-test or Welch's *t*-test) or paired *t*-test since they all followed Gaussian distribution. One-way ANOVA was used for analysis of data involving more than two groups, followed by Sidak's multiple comparisons test. For I/O curves we used Two-way repeated measures ANOVA with stimulus intensity as the repeated factor. This was followed by Sidak's multiple comparisons tests.

When possible, data from male and female animals were compared using 2-tailed parametric unpaired *t*-tests. No significant differences were found across sexes, and data from all animals were pooled together. Precise details for each experiment are found in figure legends. A value of $p \leq 0.05$ indicates statistical significance. In box-and-whisker plots, the central horizontal line denotes the median, the edges show upper and lower quartiles, the whiskers show minimum and maximum values and the points depict individual experiments. In figures, empty dots refer to female mice, while full dots to males. All other data are presented as mean ± s.e.m.

RESULTS

Midbrain lesion with 6-OHDA induces loss of dopaminergic innervation and LTP deficits in the dorsal hippocampus, as well as memory impairments

The midbrain dopaminergic inputs to the dorsal hippocampus arise from the lateral VTA and medial SNpc [6, 28]. The first part of our study sought to confirm that loss of the midbrain-hippocampus dopaminergic pathway can affect CA3-CA1 LTP. To this aim, we used 6-OHDA, a catecholaminergic neurotoxin, to selectively lesion midbrain DA neurons (thereafter, 6-OHDA mice). Two-month-old C57BL/6N mice were stereotaxically injected in the left midbrain with 6-OHDA or Saline (thereafter, Saline mice) and examined 1-month post lesion (Fig. 1A). Stereological counts of TH^+ neurons in the VTA and SNpc ipsilateral to the lesion confirmed the strong loss of DA neurons in 6-OHDA mice (Fig. 1B). Consequently, the TH^+ fibre density was significantly reduced in the hippocampus ipsilateral to the 6-OHDA lesion (Fig. 1C; see also Supplementary Fig. 1A) whereas no significant changes were detected in the total TH^+ fibre density in the contralateral hippocampus, despite a reduction in CA3 (Supplementary Fig. 1B). Consistent with the loss of hippocampal dopaminergic fibres, the HPLC analysis of ipsilateral hippocampal tissue revealed decreased levels of DA and its relative metabolites (DOPAC and HVA), in 6-OHDA-treated mice compared to Saline controls (Fig. 1D).

To prevent retrograde lesioning of LC DA-releasing neurons, 6-OHDA mice were intraperitoneally injected with the NE reuptake inhibitor desipramine before the intracranial inoculation of 6-OHDA (Fig. 1A). Stereological analysis confirmed that the number of TH^+ neurons in the ipsilateral LC was unchanged in 6-OHDA mice (Supplementary Fig. 1C), and the density of fibres expressing the NE transporter (NET) in both the total hippocampus and its subregions remained intact (Supplementary Fig. 1D). Additionally, we did not observe differences in the hippocampal levels of NE and its metabolite MOPEG (Supplementary Fig. 1E), indicating that the 6-OHDA lesion did not retrogradely affect the LC neurons.

The DA released from the VTA/SNpc to the hippocampus plays an important role in modulating hippocampal glutamatergic transmission, synaptic plasticity and memory [2, 4–6, 26]. However, this role has been questioned since the publication of works showing that the main dopaminergic innervation in the dorsal hippocampus originates from the LC and acts *via* D1/D5 receptors [3, 7, 8, 29]. To verify whether the depletion of VTA/SNpc DA neurons can induce deficits in CA3-CA1 synaptic plasticity, we measured the LTP magnitude in the dorsal hippocampus of 6-OHDA mice. Two trains of high-frequency stimulation (HFS; 2×100 Hz) induced a field EPSP (fEPSP) slope potentiation of 134 ± 8% in Saline mice, but only 114 ± 4% in 6-OHDA mice after 60 min of recording (Fig. 1E). Of note, the initial (post-tetanic) phase of HFS-LTP appeared intact in 6-OHDA mice. Instead, the late-phase of the HFS-LTP was affected by the lesion. On the other hand, the input-output relationship was similar across groups, indicating no changes in the responsiveness of the glutamatergic fibres to electrical stimulation (Supplementary Fig. 1F).

We next investigated the role of midbrain DA in the NOR test. Consistent with the reduction of dopaminergic innervation in the hippocampus, 6-OHDA-treated mice failed to discriminate between the familiar and novel objects, in contrast to Saline-treated mice that exhibited a robust preference for the novel object (Fig. 1F). These findings support the notion that midbrain derived DA is critical for spatial exploration and object recognition memory. Instead, the time spent in the centre *versus* the periphery of the arena, as well as the total distance travelled in the open field arena, remained unchanged in 6-OHDA-treated mice (Supplementary Fig. 1G, H).

Crossing of DATCre mice with the Tg2576 mouse model of AD recapitulates VTA DA neuron degeneration

In the first part of our work, through the injection of 6-OHDA, we demonstrated that midbrain DA depletion can impair hippocampal CA3-CA1 LTP. Building upon this, we sought to determine whether selective midbrain dopaminergic stimulation could restore hippocampal glutamatergic transmission and LTP deficits in the Tg2576 mouse model of AD. Our prior work has established that this mouse model exhibits selective degeneration of VTA DA neurons as early as 2–3 months of age, culminating in hippocampal neuronal and synaptic plasticity dysfunctions by 6–7 months of age [10, 12, 14, 15]. Systemic administration of dopaminergic drugs has been shown to rescue the LTP deficits in Tg2576 mice; however, such interventions may exert their effects

indirectly by modulating other brain regions functionally connected with the hippocampus [30]. We therefore sought to investigate whether selectively stimulation of the residual, non-degenerated midbrain dopaminergic fibres within the dorsal hippocampus would be sufficient to rescue LTP deficits in Tg2576 mice.

To enable precise optogenetic activation of midbrain DA neurons, while preserving the characteristic neurodegeneration and hippocampal DA depletion of naïve Tg2576 mice, we generated a modified mouse model. Heterozygous Tg2576 mice were crossed with DATCre mice, that express the Cre recombinase gene under control of the endogenous DA transporter (DAT) promoter, to obtain DATCre/Tg2576 and control littermates (DATCre/WT; Fig. 2A). In line with what reported for naïve Tg2576 mice [31], we observed that F1 DATCre/Tg2576 offspring at 6 months of age do not exhibit parenchymal Aβ plaques in the hippocampus, yet they display elevated intracellular Aβ levels compared to their DATCre/WT littermates, consistent with the AD phenotype (Fig. 2B). Stereological analysis further revealed a significant reduction in TH^+ neurons within the VTA at 6 months of age (Fig. 2C), mirroring the DA neurodegeneration previously reported in naïve Tg2576 mice [13, 15]. In agreement with this, TH^+ fibre density was also reduced in the dorsal hippocampus (Fig. 2E, Supplementary Fig. 2A). Notably, and in line with previous findings [15], DATCre/Tg2576 mice did not display degeneration of dopaminergic neurons in the SNpc (Fig. 2D).

Phasic and prolonged optogenetic stimulation of VTA/SNpc dopaminergic neurons differentially modulate DA neuron firing

The nature of midbrain DA neuron firing is such that these neurons cannot sustain prolonged high-frequency spiking, and may undergo depolarization-induced block of firing [32–34]. Therefore, optogenetic stimulation of midbrain dopaminergic neurons may induce differential results depending on the protocol of photostimulation. To establish a protocol that can maintain a sustained activation of VTA/SNpc DA neurons, but preclude depolarization block, we tested two different protocols – phasic and prolonged stimulation – in the VTA of DATCre/WT mice during recordings of spontaneous neuronal firing in acute midbrain slices. 5-month-old DATCre/WT mice received bilateral stereotaxic injections into the VTA of AAV-EF1a-DIO-hChR2(H134R)-eYFP (Fig. 2F, G). eYFP-positive immunofluorescence in parasagittal slices of 6-month-old DATCre/WT used for electrophysiological recordings confirmed the expression of the ChR2-eYFP fused protein in the midbrain TH^+ neurons (Fig. 2G), also showing slight but evident labelling of eYFP-positive fibres in the dorsal hippocampus (Fig. 2H).

Then, we performed extracellular recordings from ChR2-eYFP-expressing neurons in the lateral VTA, that projects to the dorsal hippocampus [5]. The single-unit recordings confirmed the identity of dopaminergic neurons based on their slow and regular pacemaking, with firing in the range of 1–8 Hz (Fig. 2I). In these neurons, we applied both a phasic and a prolonged photostimulation protocol: the first one was a burst of three 5-ms long light pulses at 66.66 Hz (15 ms interval) administered for 25 times, while the second protocol consisted of a single, continuous 800 ms-long light pulse. As shown in Fig. 2I, the phasic protocol synchronized the firing of VTA DA neurons and allowed a rapid recovery of pacemaking activity right after photostimulation. Conversely, the prolonged protocol induced an initial burst firing that was followed by long-lasting neuron silencing, indicating that this protocol could not be used for reliable DA neuron excitation. Based on these results, we decided to use the phasic optogenetic stimulation for the following experiments.

The phasic optogenetic stimulation of hippocampal dopaminergic fibres potentiates the CA3-CA1 synaptic transmission and rescues LTP in Tg2576 mice

We next performed optogenetic stimulation of VTA/SNpc dopaminergic fibres in the dorsal hippocampus to investigate whether the activation of the midbrain-hippocampus dopaminergic pathway is sufficient to rescue glutamatergic synaptic deficits in CA3-CA1 synapses of Tg2576 mice. We first delivered the phasic photostimulation protocol in DATCre/WT and DATCre/Tg2576 hippocampal slices during basal electrical stimulation of the Schaffer collaterals with single square pulses (Fig. 3A). We observed that the photostimulation induced an increase in the slope of fEPSPs in both experimental groups, which developed progressively over at least 30 min (Fig. 3B). Notably, this form of synaptic plasticity did not require HFS and was much more pronounced in DATCre/WT ($157 \pm 12\%$) compared to DATCre/Tg2576 slices ($123 \pm 5\%$; Fig. 3B). This smaller effect in DATCre/Tg2576 mice was not surprising given the reduced hippocampal dopaminergic innervation in 6-month-old DATCre/Tg2576. Yet, the potentiation of fEPSPs from DATCre/Tg2576 mice was clearly mediated by midbrain DA as the effect of photostimulation was blocked by the presence of bath-applied SCH-23390, a D1/D5 receptor antagonist. Indeed, SCH-23390 completely prevented the effect of photostimulation on fEPSP and induced a mild, yet significant depression of responses compared to baseline (Fig. 3B). These results confirm that midbrain DA can effectively potentiate the CA3-CA1 glutamatergic transmission in DATCre/Tg2576 mice, despite the reduced dopaminergic innervation in the Tg2576 hippocampus.

We next examined the ability of phasic dopaminergic photostimulation to rescue CA3-CA1 synaptic plasticity dysfunctions in DATCre/Tg2576 mice. In absence of optogenetic stimulation (Sham condition), DATCre/Tg2576 mice show pronounced deficits in HFS-induced synaptic plasticity (HFS-LTP) in comparison to DATCre/WT mice (Fig. 3C; Supplementary Fig. 2B), confirming our previous results from naïve Tg2576 mice [15]. Instead, the dopaminergic fibre photostimulation (Opto condition), applied just before the two HFS trains, could fully rescue HFS-LTP in DATCre/Tg2576 Opto mice (Fig. 3C). Notably, the photostimulation did not further increase HFS-LTP in DATCre/WT mice (Supplementary Fig. 2C).

Taken together, our data demonstrate that the phasic optogenetic stimulation of VTA/SNpc-derived dopaminergic fibres in the hippocampus of Tg2576 mice potentiates the glutamatergic CA3-CA1 synaptic transmission and rescues plasticity dysfunctions.

DISCUSSION

Using opposing approaches applied to C57BL/6N mice and to the Tg2576 mouse model of AD, this study provides direct evidence that VTA/SNpc DA neurons are crucial for dorsal hippocampus-dependent plasticity. On one hand, the selective lesion of these neurons, induced by 6-OHDA, indicates the importance of midbrain DA for hippocampal HFS-LTP and memory performance. On the other hand, the direct optogenetic excitation of the midbrain-hippocampal pathway in Tg2576 mice proves that DA is both necessary and sufficient to restore glutamatergic transmission and rescue plasticity dysfunctions associated with VTA neurodegeneration in the context of AD.

This work indicates that the 6-OHDA-driven depletion of midbrain dopaminergic neurons causes a reduction of HFS-LTP in the CA1 region of C57BL/6N mice, in line with earlier works performed in vivo or in brain slices [35, 36]. Further, we observed deficits in NOR memory, in line with the importance of midbrain DA in memory performances. Notably, the neurotoxin did not affect TH^+ neurons in the LC, indicating a targeted effect on midbrain DA neurons. Of note, the loss of hippocampal HFS-LTP in

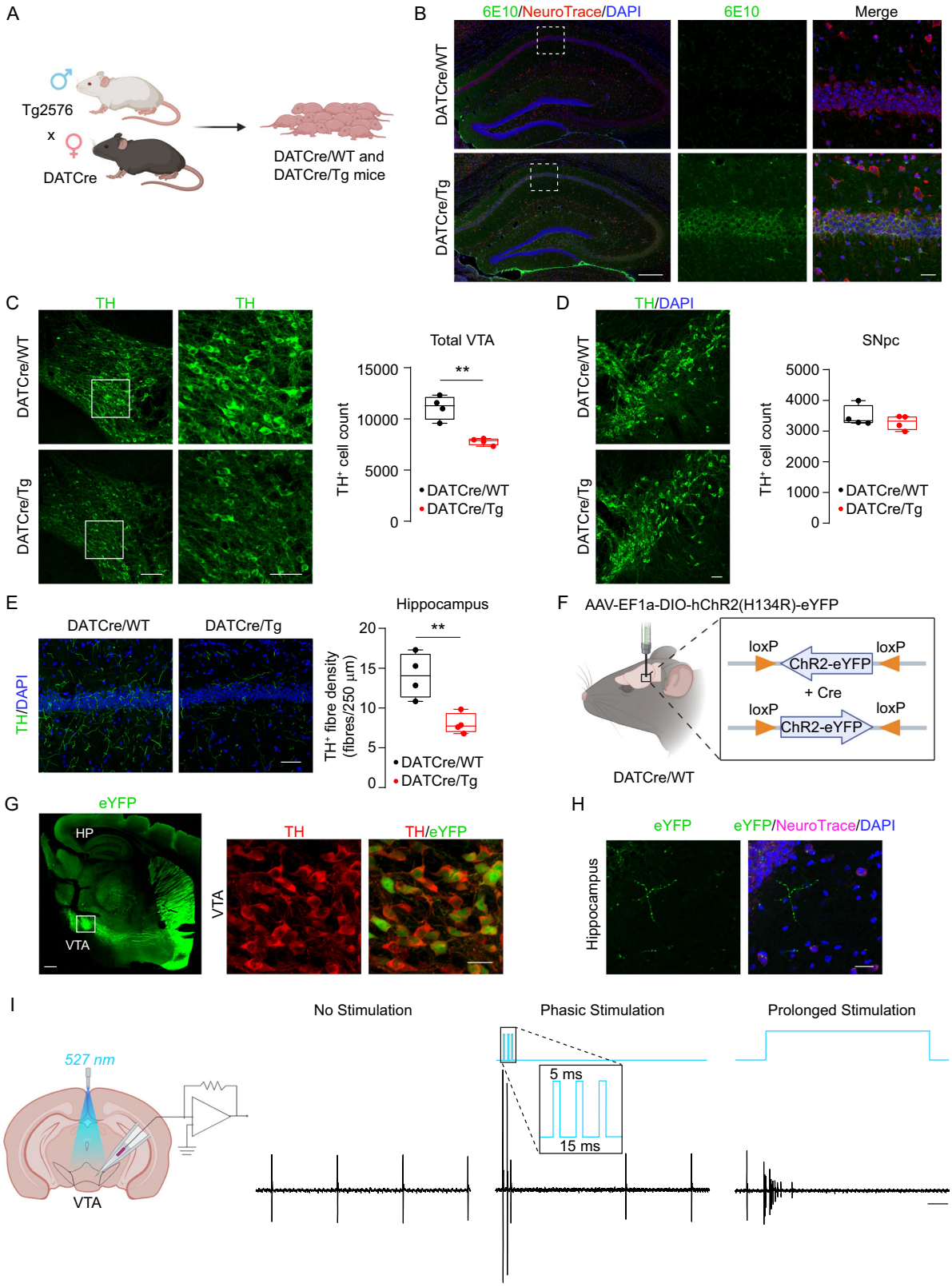

6-OHDA mice might result indirectly from DA deprivation in brain regions that regulate hippocampal pyramidal neuron activity, including the amygdala, ventral hippocampus and prefrontal cortex. Although we cannot entirely rule out that impairments in NOR memory in these mice may be influenced by motor deficits due to lesioning of the SNpc DA neurons, potentially affecting object interaction and encoding, the absence of significant differences in the total distance travelled in the open field test argues against the presence of substantial locomotor impairments. Importantly, the observed reduction of TH^+ innervation

Fig. 2 Validation of DATCre-Tg2576 model, a new mouse model for optogenetic stimulation of VTA in 6-month-old Tg2576 mice. **A** Heterozygous DATCre female mice were crossed with heterozygous Tg2576 males to obtain DATCre/WT and DATCre/Tg2576 (Tg) mice for optogenetic stimulation of VTA DA neurons. **B** 6E10 immunostaining of intracellular Aβ levels in the hippocampus of 6-month-old DATCre/WT and DATCre/Tg2576 mice. Nuclei are counterstained with DAPI and neurons with NeuroTrace (scale: 250 µm; inset 25 µm). **C-D** Representative coronal sections of the midbrain showing immunofluorescence for TH^+ neurons in DATCre/WT and DATCre/Tg mice at 6 months of age (n = 4 mice / group; scale bar: 100 µm; inset 50 µm) and stereological TH^+ cell count in total VTA (Unpaired *t*-test: **p = 0.0015) and unilateral SNpc (**D**; scale bar: 50 µm). **E** Confocal images and plot showing TH^+ fibre density (expressed as fibres / 250 µm; scale bar: 50 µm) in the dorsal hippocampus of DATCre/WT and DATCre/Tg mice at 6 months of age (n = 4 mice / group. Unpaired *t*-test: **p = 0.0080). Nuclei are counterstained with DAPI. **F** 5-month-old DATCre/WT mice were bilaterally infused in the midbrain with AAV-EF1a-DIO-hChR2(H134R)-eYFP for selective expression of the ChR2-eYFP fused protein in the mouse midbrain. Mice were used for experiments 1-month post-injection. **G** Representative confocal images show eYFP fluorescence in a brain slice used for electrophysiology. The square indicates the midbrain (scale bar: 500 µm). The images on the right show the co-labelling of eYFP and TH (scale bar: 10 µm). **H** Representative confocal images of eYFP fluorescence in the dorsal hippocampus of a 6-month-old DATCre/WT mouse injected with the viral construct in the midbrain (scale bar: 25 µm). Nuclei are counterstained with DAPI and neurons with NeuroTrace. **I** Schematic representation of optogenetic stimulation of dopaminergic ($eYFP^+$) neurons in VTA of 6-month-old DATCre/WT applied during electrophysiology recordings. Representative traces of spontaneous firing of a DA neuron in the lateral VTA at 6 months of age before photostimulation, and during phasic (shown in detail in the inset) and prolonged light stimulation (scale bar: 100 ms). Note how the spontaneous pacemaking activity is restored following the end of phasic stimulation, but the neuron remains silent during the prolonged stimulation. [Schematics were created using BioRender (https://biorender.com)].

within the hippocampus, alongside the decreased DA levels following 6-OHDA, support the notion that HFS-LTP and memory impairments are a direct consequence of local DA loss. Interestingly, our results show that only the late phase of the HFS-LTP was affected by the lesion, leaving intact the early post-tetanic phase. This is in agreement with previous works showing that D1/D5 receptor antagonists can spare the early phase of LTP while blocking the late phase, a process associated with de novo protein synthesis downstream of dopaminergic signalling [2, 37–39].

Additionally, our results provide further insights into the regulation of midbrain DA neuron firing under external manipulations; this knowledge should be taken into consideration when chemogenic or optogenetic stimulation is used in experimental settings. Indeed, we showed that prolonged DA neuron activation by optogenetic stimulation is unable to maintain neuronal firing, probably due to over-excitation and depolarization block. Similarly, others observed that chronic chemogenetic DA neuron stimulation in a mouse model of Parkinson's Disease paradoxically leads to a decline in motor function, while chronic inhibition increases locomotor activity [40–42]. Conversely, the phasic optogenetic stimulation effectively synchronized firing to the light pulses, mimicking the natural bursting activity of midbrain DA neurons, while allowing a prompt recovery of pacemaking activity when photostimulation was over. A similar phasic photostimulation protocol on hippocampal midbrain-derived dopaminergic fibres had been useful for studying the precise role of midbrain DA for place preference, contextual memory encoding and spatial memory persistence, and for deciphering how the midbrain controls hippocampal excitatory glutamatergic transmission in CA3-CA1 synapses [4, 5, 26, 43].

To our knowledge, this study provides the first demonstration that selective activation of the midbrain dopaminergic pathway modulates the hippocampal glutamatergic transmission in the context of AD. While previous studies, including our own, have shown that dopaminergic drugs rescue neuronal and plasticity deficits in AD mouse models [14, 15, 20], direct evidence that targeted activation of midbrain DA neurons alone is sufficient to elicit such rescue was lacking. Here, we show that DA release from VTA/SNpc upon phasic optogenetic stimulation is both necessary and sufficient to potentiate CA3-CA1 glutamatergic transmission and fully restore HFS-LTP deficits in Tg2576 mice. The present work builds upon our previous findings showing that LTP deficits in 6-month-old Tg2576 mice are strictly correlated with the early and selective degeneration of DA neurons in the VTA since 2–3 months, in contrast to SNpc and LC neurons that remain intact [15], suggesting a higher vulnerability of VTA DA neurons. Our new findings indicate that, despite the ongoing degeneration in the VTA and the reduced anatomical connectivity with the hippocampus, the remaining neurons can be functionally recruited to compensate for the loss of DA, thus engaging in plasticity mechanisms in the dorsal hippocampus.

Our findings align with the emerging concept that the dopaminergic input from the VTA can elicit "DA-LTP", a form of LTP characterized by enhanced CA3-CA1 glutamatergic transmission in the absence of HFS or other classical electrical LTP-inducing paradigms [5]. Consistent with previous reports [26], we demonstrate that DA-LTP can be fully prevented by the D1/D5 receptor antagonist SCH-23390, thereby confirming that this HFS-independent form of potentiation is mediated by phasic DA release acting on D1/D5 receptors in CA1 pyramidal neurons. Notably, the slow progression of DA-LTP and the absence of post-tetanic potentiation further support the involvement of D1/D5 receptors, as similar slow-onset potentiation can be induced by direct hippocampal infusion of D1/D5 receptor agonists [44, 45]. Of note, the potentiation we observed was largely lower in DATCre/Tg2576 mice, in line with the degeneration of most dopaminergic fibres innervating the hippocampus. Yet, it was sufficient to induce a mild potentiation that, when combined with HFS, could completely rescue HFS-LTP in these mice.

The ability of phasic dopaminergic stimulation to increase the HFS-LTP in Tg2576 mice is in striking contrast to the lack of HFS-LTP increase in WT mice. It is likely that, in non-AD conditions, the LTP is already saturated by the phasic DA released by photostimulation, and the subsequent tetanic stimulation cannot induce further increase in synaptic response. This is in agreement with the experiments of Sayegh et al., showing that their DA-LTP occluded further plasticity triggered by theta-burst stimulation, indicating a 'saturability' of the LTP phenomenon, which the authors explained as the result of common mechanisms of potentiation by DA and theta-burst stimulation [5]. In Tg2576 mice, in absence of photostimulation, the low basal DA levels do not permit the potentiation of synaptic responses, resulting in HFS-LTP deficits even though the Schaffer collaterals are normally responsive to electrical stimulation (see unchanged input-output curve between DATCre/WT and DATCre/Tg2576 sham mice; Supplementary Fig. 2B). In contrast, the photostimulation in these mice permits full recovery of HFS-LTP, further proving the necessity of DA for this process.

Notably, our work does not challenge the established role of LC-derived DA in normal hippocampal synaptic plasticity, nor does it downplay the contribution of LC deficits to AD progression. Numerous studies have demonstrated the importance of LC-derived hippocampal DA in regulating attention, memory retrieval, contextual memory linking and spatial memory, even in the absence of reward [7–12]. Consistent with these functions, LC deficits (i.e., functional disconnection with cortical regions, tau

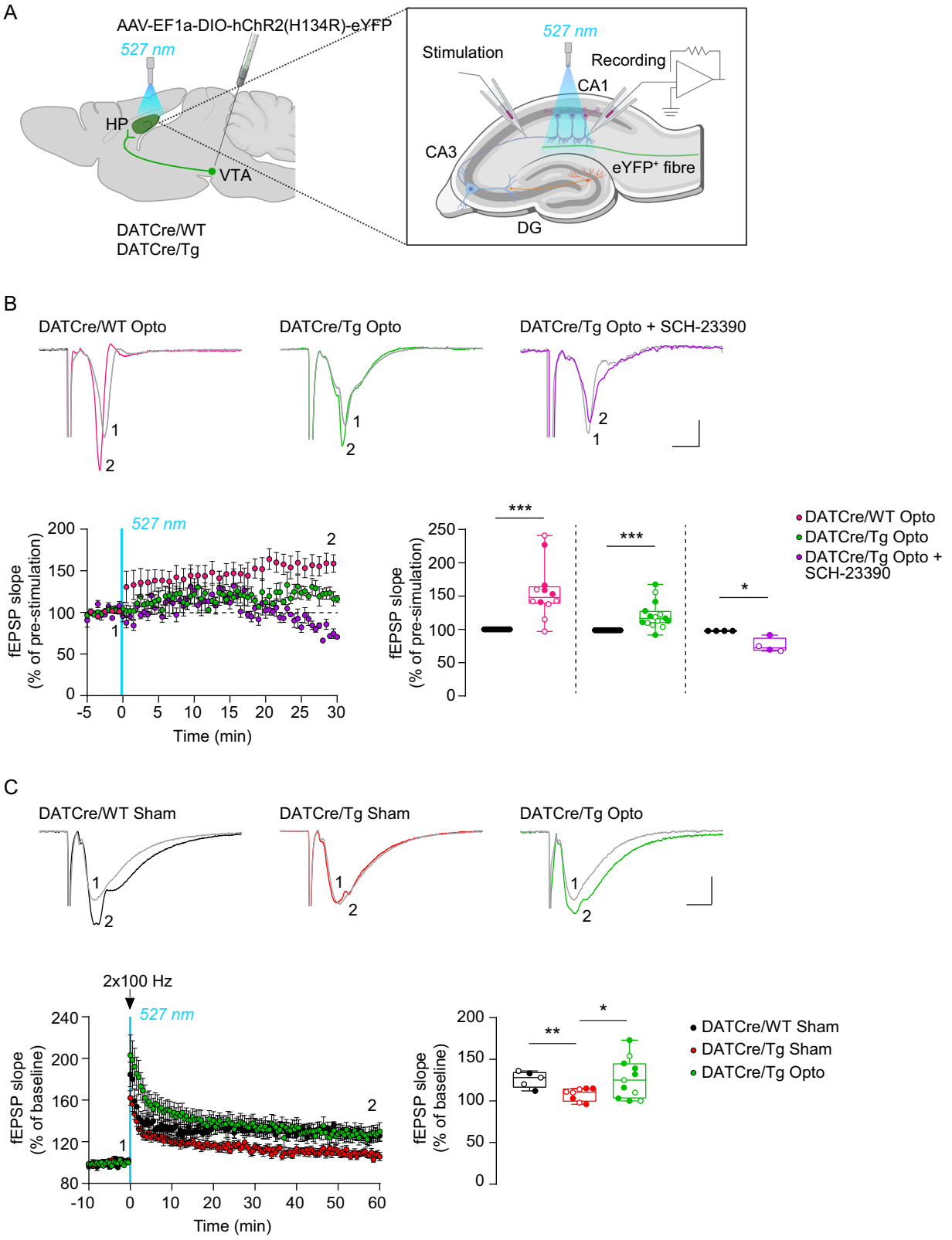

tangle accumulation and/or neuronal degeneration) have been implicated since the early phases of clinical AD [46–51] and may contribute to disease progression [52, 53]. Nonetheless, our previous work in the Tg2576 mouse model has shown that the number of LC TH$^+$ neurons, as well as the noradrenergic outflow in the hippocampus, remain intact at least up to 6 months of age. This stands in sharp contrast to the VTA, which degenerates earlier [15]. Therefore, based on these previous findings, investigating the effect of LC stimulation on synaptic plasticity in Tg2576 mice falls outside the scope of the present study.

Fig. 3 Ex-vivo optogenetic stimulation of hippocampal dopaminergic fibres induces a D1/D5 receptor-mediated potentiation of CA3-CA1 synaptic transmission and rescues HFS-LTP in 6-month-old Tg2576 mice. A Schematic representation of optogenetic stimulation of dopaminergic (eYFP^{+}) fibres in the hippocampus of 6-month-old DATCre/WT and DATCre/Tg mice applied during electrical single-pulse or HFS of Schaffer collaterals. Field EPSPs (fEPSPs) were recorded in the CA1 *stratum radiatum*. **B** Representative traces of fEPSPs (scale bar: 4 ms; 0.4 mV) from 6-month-old DATCre/WT, DATCre/Tg and DATCre/Tg mice in the presence of 20 μM SCH-23390 elicited in the dorsal hippocampus at half maximal Schaffer collateral stimulation before (1) and 30 min after (2) dopaminergic phasic photostimulation (depicted by the blue vertical band). The plots below show the time-course and pooled data of the average fEPSP slope (± s.e.m.) normalized to the mean fEPSP slope pre-stimulation (DATCre/WT: n = 12 slices / 5 mice, Welch's *t*-test: ***p = 0.0005; DATCre/Tg: n = 15 slices / 10 mice, Welch's *t*-test: ***p = 0.0003, DATCre/Tg SCH23390: n = 4 slices / 3 mice, Welch's *t*-test: *p = 0.0275). Empty dots refer to female mice, while full dots to males. **C** Representative traces (scale bar: 10 ms; 1 mV) showing fEPSPs elicited in the dorsal hippocampus at half maximal Schaffer collateral stimulation in DATCre/WT and DATCre/Tg slices from 6-month-old mice during baseline (1) and 1 h (2) after two HFS trains. The phasic optogenetic stimulation protocol (blue band) was applied just prior to the HFS trains (vertical arrow) in DATCre/Tg slices (Opto mice) and was compared to DATCre/WT and DATCre/Tg mice not receiving photostimulation (Sham mice). The plot below shows the time-course of normalized, average fEPSP slope and the pooled data (DATCre/WT Sham: n = 5 slices / 3 mice; DATCre/Tg Sham: n = 8 slices / 3 mice; DATCre/Tg Opto: n = 11 slices / 4 mice; One-Way ANOVA for treatment and genotype $F_{2,21} = 3.8190$, p = 0.0385; DATCre/WT Sham vs DATCre/Tg Sham: **p = 0.0034; DATCre/Tg Sham vs DATCre/Tg Opto: *p = 0.0493 with Sidak's multiple comparisons test). Empty dots refer to female mice, while full dots to males. [Schematics were created using BioRender (https://biorender.com)].

Our findings hold significant clinical implications, particularly in light of the growing recognition of midbrain dopaminergic dysfunction as a critical contributor to AD pathology from its earliest stages. Emerging evidence underscores the strong association between the VTA integrity and hippocampal function, with structural and functional connectivity of the VTA correlating with cognitive performance in healthy individuals [54, 55]. Notably, the mesocorticolimbic dopaminergic circuit exhibits early vulnerability in AD, as indicated by VTA atrophy, reduced functional VTA connectivity with target areas, hypometabolism and neuroinflammatory changes within mesocorticolimbic brain targets [54–63]. Indeed, disruptions in mesocorticolimbic pathways are detectable as early as the mild cognitive impairment (MCI) stage and are associated with an accelerated transition from MCI to dementia [23, 55, 56, 58, 60–66].

Our findings in the Tg2576 model indicate that selectively enhancing the midbrain dopaminergic signalling may constitute a novel therapeutic strategy that can work as an alternative to systemic pharmacological interventions. As such, this circuit-specific approach may offer advantages over traditional, systemic DA-replacement therapies that lack anatomical precision and often induce important off-target effects. Indeed, while systemic administration of L-DOPA or other DA-enhancing agents may be advantageous against motor, cognitive or motivational deficits, the non-selective and widespread activation of DA circuits frequently results in adverse effects (i.e. psychomotor agitation, autonomic nervous system dysregulation, mood changes and altered reward processing). These complications reflect the indiscriminate stimulation of both vulnerable and intact DA pathways. In Parkinson's Disease, DA neuron loss predominantly affects the nigrostriatal pathway, yet systemic DA therapies also activate relatively preserved mesocorticolimbic projections to the prefrontal and occipital cortex, Nucleus Accumbens and hippocampus from the VTA. This off-target stimulation contributes to well-known complications like impulse control disorders, disinhibition, and levodopa-induced dyskinesia.

In an even manner, the nigrostriatal pathway remains largely preserved in the prodromal and MCI stages of AD, despite the early vulnerability of the mesocorticolimbic dopaminergic circuit. Accordingly, systemic DA enhancement in this context may lead to overactivation of circuits involved in motor control, potentially precipitating extrapyramidal signs or disrupting homeostasis within the basal ganglia.

Although optogenetic approaches provide key insights into the functional connectivity and behavioral relevance of VTA hippocampal projections, their translational applicability is limited. In this context, non-invasive neuromodulatory techniques with growing clinical applicability such as transcranial electrical, magnetic stimulation or vagal nerve stimulation have shown efficacy in improving cognitive function in AD [67–70]. These interventions are thought to exert their beneficial effects by modulating mesocorticolimbic DA circuits, thereby restoring hippocampal synaptic plasticity and cognitive resilience [71]. In line with this notion, we have recently shown that transcranial direct current stimulation (tDCS) selectively increases the excitability of VTA DA neurons, enhances hippocampal DA release and potentiates LTP without inducing widespread dopaminergic activation [72]. These effects were associated with improved memory, attenuated microglia-mediated neuroinflammation and significant reduction in amyloid load. Such an approach may be well-suited for individuals with MCI or early AD. By preferentially engaging vulnerable mesocorticolimbic circuits in AD, tDCS offers a targeted, safer means of modulating synaptic plasticity and cognitive function. Ultimately, such circuit-level precision may not only avoid the off-target effects seen with conventional DA therapies but also provide a means toward slowing disease progression through selective neuromodulatory engagement.

DATA AVAILABILITY

All data are available in the main or supplementary files. Raw data can be freely-available by the corresponding author upon request.

REFERENCES

1. Russo SJ, Nestler EJ. The brain reward circuitry in mood disorders. Nat Rev Neurosci. 2013;14:609–25.
2. Broussard JI, Yang K, Levine AT, Tsetsenis T, Jenson D, Cao F, et al. Dopamine regulates aversive contextual learning and associated in vivo synaptic plasticity in the hippocampus. Cell Rep. 2016;14:1930–9.
3. Hagena H, Manahan-Vaughan D. Oppositional and competitive instigation of hippocampal synaptic plasticity by the VTA and locus coeruleus. Proc Natl Acad Sci USA. 2025;122:e2402356122.
4. McNamara CG, Tejero-Cantero Á, Trouche S, Campo-Urriza N, Dupret D. Dopaminergic neurons promote hippocampal reactivation and spatial memory persistence. Nat Neurosci. 2014;17:1658–60.
5. Sayegh FJP, Mouledous L, Macri C, Pi Macedo J, Lejards C, Rampon C, et al. Ventral tegmental area dopamine projections to the hippocampus trigger long-term potentiation and contextual learning. Nat Commun. 2024;15:4100.
6. Tsetsenis T, Badyna JK, Wilson JA, Zhang X, Krizman EN, Subramaniyan M, et al. Midbrain dopaminergic innervation of the hippocampus is sufficient to modulate formation of aversive memories. Proc Natl Acad Sci USA. 2021;118:e2111069118.
7. Kempadoo KA, Mosharov EV, Choi SJ, Sulzer D, Kandel ER. Dopamine release from the locus coeruleus to the dorsal hippocampus promotes spatial learning and memory. Proc Natl Acad Sci. 2016;113:14835–40.
8. Takeuchi T, Duszkiewicz AJ, Sonneborn A, Spooner PA, Yamasaki M, Watanabe M, et al. Locus coeruleus and dopaminergic consolidation of everyday memory. Nature. 2016;537:357–62.
9. Smith CC, Greene RW. CNS dopamine transmission mediated by noradrenergic innervation. J Neurosci. 2012;32:6072–80.

10. Spoleti E, La Barbera L, Cauzzi E, De Paolis ML, Saba L, Marino R, et al. Dopamine neuron degeneration in the Ventral Tegmental Area causes hippocampal hyperexcitability in experimental Alzheimer's disease. Mol Psychiatry. 2024;29:1265–80.
11. La Barbera L, Nobili A, Cauzzi E, Paoletti I, Federici M, Saba L, et al. Upregulation of Ca2+-binding proteins contributes to VTA dopamine neuron survival in the early phases of Alzheimer's disease in Tg2576 mice. Mol Neurodegener. 2022;17:76.
12. Spoleti E, Krashia P, La Barbera L, Nobili A, Lupascu CA, Giacalone E, et al. Early derailment of firing properties in CA1 pyramidal cells of the ventral hippocampus in an Alzheimer's disease mouse model. Exp Neurol. 2022;350:113969.
13. La Barbera L, Vedele F, Nobili A, Krashia P, Spoleti E, Latagliata EC, et al. Nilotinib restores memory function by preventing dopaminergic neuron degeneration in a mouse model of Alzheimer's disease. Prog Neurobiol. 2021;202:102031.
14. Cordella A, Krashia P, Nobili A, Pignataro A, La Barbera L, Viscomi MT, et al. Dopamine loss alters the hippocampus-nucleus accumbens synaptic transmission in the Tg2576 mouse model of Alzheimer's disease. Neurobiol Dis. 2018;116:142–54.
15. Nobili A, Latagliata EC, Viscomi MT, Cavallucci V, Cutuli D, Giacovazzo G, et al. Dopamine neuronal loss contributes to memory and reward dysfunction in a model of Alzheimer's disease. Nat Commun. 2017;8:14727.
16. Cavallucci V, Ferraina C, D'Amelio M. Key role of mitochondria in Alzheimer's disease synaptic dysfunction. Curr Pharm Des. 2013;19:6440–50.
17. Hao J-R, Sun N, Lei L, Li X-Y, Yao B, Sun K, et al. L-Stepholidine rescues memory deficit and synaptic plasticity in models of Alzheimer's disease via activating dopamine D1 receptor/PKA signaling pathway. Cell Death Dis. 2015;6:e1965.
18. Guzmán-Ramos K, Moreno-Castilla P, Castro-Cruz M, McGaugh JL, Martínez-Coria H, LaFerla FM, et al. Restoration of dopamine release deficits during object recognition memory acquisition attenuates cognitive impairment in a triple transgenic mice model of Alzheimer's disease. Learn Mem Cold Spring Harb N. 2012;19:453–60.
19. Himeno E, Ohyagi Y, Ma L, Nakamura N, Miyoshi K, Sakae N, et al. Apomorphine treatment in Alzheimer mice promoting amyloid-β degradation. Ann Neurol. 2011;69:248–56.
20. Jürgensen S, Antonio LL, Mussi GEA, Brito-Moreira J, Bomfim TR, De Felice FG, et al. Activation of D1/D5 dopamine receptors protects neurons from synapse dysfunction induced by amyloid-beta oligomers. J Biol Chem. 2011;286:3270–6.
21. Ambrée O, Richter H, Sachser N, Lewejohann L, Dere E, de Souza Silva MA, et al. Levodopa ameliorates learning and memory deficits in a murine model of Alzheimer's disease. Neurobiol Aging. 2009;30:1192–204.
22. Gálvez-Márquez DK, Salgado-Ménez M, Moreno-Castilla P, Rodríguez-Durán L, Escobar ML, Tecuapetla F, et al. Spatial contextual recognition memory updating is modulated by dopamine release in the dorsal hippocampus from the locus coeruleus. Proc Natl Acad Sci USA. 2022;119:e2208254119.
23. Krashia P, Spoleti E, D'Amelio M. The VTA dopaminergic system as diagnostic and therapeutical target for Alzheimer's disease. Front Psychiatry. 2022;13:1039725.
24. Paxinos G, Franklin KBJ. Paxinos and Franklin's the Mouse Brain in Stereotaxic Coordinates. 5th Edition. Elsevier/Academic Press; 2019.
25. Guatteo E, Rizzo FR, Federici M, Cordella A, Ledonne A, Latini L, et al. Functional alterations of the dopaminergic and glutamatergic systems in spontaneous α-synuclein overexpressing rats. Exp Neurol. 2017;287:21–33.
26. Rosen ZB, Cheung S, Siegelbaum SA. Midbrain dopamine neurons bidirectionally regulate CA3-CA1 synaptic drive. Nat Neurosci. 2015;18:1763–71.
27. Krashia P, Martini A, Nobili A, Aversa D, D'Amelio M, Berretta N, et al. On the properties of identified dopaminergic neurons in the mouse substantia nigra and ventral tegmental area. Eur J Neurosci. 2017;45:92–105.
28. Gasbarri A, Verney C, Innocenzi R, Campana E, Pacitti C. Mesolimbic dopaminergic neurons innervating the hippocampal formation in the rat: a combined retrograde tracing and immunohistochemical study. Brain Res. 1994;668:71–79.
29. McNamara CG, Dupret D. Two sources of dopamine for the hippocampus. Trends Neurosci. 2017;40:383–4.
30. Lisman JE, Grace AA. The Hippocampal-VTA Loop: controlling the entry of information into long-term memory. Neuron. 2005;46:703–13.
31. Hsiao K, Chapman P, Nilsen S, Eckman C, Harigaya Y, Younkin S, et al. Correlative memory deficits, Abeta elevation, and amyloid plaques in transgenic mice. Science. 1996;274:99–102.
32. Richards CD, Shiroyama T, Kitai ST. Electrophysiological and immunocytochemical characterization of GABA and dopamine neurons in the substantia nigra of the rat. Neuroscience. 1997;80:545–57.
33. Yung WH, Häusser MA, Jack JJ. Electrophysiology of dopaminergic and non-dopaminergic neurones of the guinea-pig substantia nigra pars compacta in vitro. J Physiol. 1991;436:643–67.
34. Grace AA, Bunney BS. Nigral dopamine neurons: intracellular recording and identification with L-Dopa injection and histofluorescence. Science. 1980;210:654–6.
35. Costa C, Sgobio C, Siliquini S, Tozzi A, Tantucci M, Ghiglieri V, et al. Mechanisms underlying the impairment of hippocampal long-term potentiation and memory in experimental Parkinson's disease. Brain J Neurol. 2012;135:1884–99.
36. Esmaeili-Mahani S, Haghparast E, Nezhadi A, Abbasnejad M, Sheibani V. Apelin-13 prevents hippocampal synaptic plasticity impairment in Parkinsonism rats. J Chem Neuroanat. 2021;111:101884.
37. Lemon N, Manahan-Vaughan D. Dopamine D1/D5 receptors gate the acquisition of novel information through hippocampal long-term potentiation and long-term depression. J Neurosci Off J Soc Neurosci. 2006;26:7723–9.
38. Frey U, Huang YY, Kandel ER. Effects of cAMP simulate a late stage of LTP in hippocampal CA1 neurons. Science. 1993;260:1661–4.
39. Fuchsberger T, Stockwell I, Woods M, Brzosko Z, Greger IH, Paulsen O. Dopamine increases protein synthesis in hippocampal neurons enabling dopamine-dependent LTP. eLife. 2025;13:RP100822.
40. Chohan MO, Fein H, Mirro S, O'Reilly KC, Veenstra-VanderWeele J. Repeated chemogenetic activation of dopaminergic neurons induces reversible changes in baseline and amphetamine-induced behaviors. Psychopharmacology (Berl). 2023;240:2545–60.
41. Salesse C, Charest J, Doucet-Beaupré H, Castonguay A-M, Labrecque S, De Koninck P, et al. Opposite control of excitatory and inhibitory synapse formation by Slitrk2 and Slitrk5 on dopamine neurons modulates hyperactivity behavior. Cell Rep. 2020;30:2374–2386.e5.
42. Torre-Muruzabal T, Devoght J, Van den Haute C, Brône B, Van der Perren A, Baekelandt V. Chronic nigral neuromodulation aggravates behavioral deficits and synaptic changes in an α-synuclein based rat model for Parkinson's disease. Acta Neuropathol Commun. 2019;7:160.
43. Tsai H-C, Zhang F, Adamantidis A, Stuber GD, Bonci A, de Lecea L, et al. Phasic firing in dopaminergic neurons is sufficient for behavioral conditioning. Science. 2009;324:1080–4.
44. Navakkode S, Sajikumar S, Frey JU. Synergistic requirements for the induction of dopaminergic D1/D5-receptor-mediated LTP in hippocampal slices of rat CA1 in vitro. Neuropharmacology. 2007;52:1547–54.
45. Navakkode S, Sajikumar S, Sacktor TC, Frey JU. Protein kinase Mζ is essential for the induction and maintenance of dopamine-induced long-term potentiation in apical CA1 dendrites. Learn Mem. 2010;17:605–11.
46. Braak H, Del Tredici K. Alzheimer's pathogenesis: is there neuron-to-neuron propagation? Acta Neuropathol (Berl). 2011;121:589–95.
47. Braak H, Thal DR, Ghebremedhin E, Del Tredici K. Stages of the pathologic process in Alzheimer disease: age categories from 1 to 100 years. J Neuropathol Exp Neurol. 2011;70:960–9.
48. Kelly SC, He B, Perez SE, Ginsberg SD, Mufson EJ, Counts SE. Locus coeruleus cellular and molecular pathology during the progression of Alzheimer's disease. Acta Neuropathol Commun. 2017;5:8.
49. Jacobs HIL, Becker JA, Kwong K, Engels-Domínguez N, Prokopiou PC, Papp KV, et al. In vivo and neuropathology data support locus coeruleus integrity as indicator of Alzheimer's disease pathology and cognitive decline. Sci Transl Med. 2021;13:eabj2511.
50. Jacobs HIL, Wiese S, van de Ven V, Gronenschild EHBM, Verhey FRJ, Matthews PM. Relevance of parahippocampal-locus coeruleus connectivity to memory in early dementia. Neurobiol Aging. 2015;36:618–26.
51. Marcyniuk B, Mann DM, Yates PO. The topography of cell loss from locus caeruleus in Alzheimer's disease. J Neurol Sci. 1986;76:335–45.
52. Heneka MT, Nadrigny F, Regen T, Martinez-Hernandez A, Dumitrescu-Ozimek L, Terwel D, et al. Locus ceruleus controls Alzheimer's disease pathology by modulating microglial functions through norepinephrine. Proc Natl Acad Sci USA. 2010;107:6058–63.
53. Liu Y, Yoo M-J, Savonenko A, Stirling W, Price DL, Borchelt DR, et al. Amyloid pathology is associated with progressive monoaminergic neurodegeneration in a transgenic mouse model of Alzheimer's disease. J Neurosci Off J Soc Neurosci. 2008;28:13805–14.
54. D'Amelio M, Serra L, Bozzali M. Ventral tegmental area in prodromal Alzheimer's Disease: bridging the gap between mice and humans. J Alzheimers Dis JAD. 2018;63:181–3.
55. De Marco M, Venneri A. Volume and connectivity of the ventral tegmental area are linked to neurocognitive signatures of Alzheimer's disease in humans. J Alzheimers Dis JAD. 2018;63:167–80.
56. Iaccarino L, Sala A, Caminiti SP, Presotto L, Perani D, Alzheimer's Disease Neuroimaging Initiative. In vivo MRI structural and PET metabolic connectivity study of dopamine pathways in Alzheimer's disease. J Alzheimers Dis JAD. 2020;75:1003–16.
57. Krashia P, Nobili A, D'Amelio M. Unifying hypothesis of dopamine neuron loss in neurodegenerative diseases: focusing on Alzheimer's disease. Front Mol Neurosci. 2019;12:123.
58. Manca R, Valera-Bermejo JM, Venneri A, Alzheimer's disease Neuroimaging Initiative. Accelerated atrophy in dopaminergic targets and medial temporo-parietal regions precedes the onset of delusions in patients with Alzheimer's disease. Eur Arch Psychiatry Clin Neurosci. 2023;273:229–41.
59. Possemato E, La Barbera L, Nobili A, Krashia P, D'Amelio M. The role of dopamine in NLRP3 inflammasome inhibition: Implications for neurodegenerative diseases. Ageing Res Rev. 2023;87:101907.

60. Sala A, Caminiti SP, Presotto L, Pilotto A, Liguori C, Chiaravalloti A, et al. In vivo human molecular neuroimaging of dopaminergic vulnerability along the Alzheimer's disease phases. Alzheimers Res Ther. 2021;13:187.
61. Serra L, D'Amelio M, Esposito S, Di Domenico C, Koch G, Marra C, et al. Ventral tegmental area disconnection contributes two years early to correctly classify patients converted to Alzheimer's disease: implications for treatment. J Alzheimers Dis JAD. 2021;82:985–1000.
62. Serra L, D'Amelio M, Di Domenico C, Dipasquale O, Marra C, Mercuri NB, et al. In vivo mapping of brainstem nuclei functional connectivity disruption in Alzheimer's disease. Neurobiol Aging. 2018;72:72–82.
63. Venneri A, De Marco M. Reduced monoaminergic nuclei MRI signal detectable in pre-symptomatic older adults with future memory decline. Sci Rep. 2020;10:18707.
64. Manca R, De Marco M, Soininen H, Ruffini L, Venneri A. Changes in neurotransmitter-related functional connectivity along the Alzheimer's disease continuum. Brain Commun. 2025;7:fcaf008.
65. Pilotto A, Galli A, Sala A, Caminiti SP, Presotto L, Liguori C. et al. Dopaminergic deficits along the spectrum of Alzheimeras disease. Mol Psychiatry. 2025;30:3069–3076.
66. Zhang Y, Liang Y, Gu Y. The dopaminergic system and Alzheimer's disease. Neural Regen Res. 2025;20:2495–512.
67. Brougher J, Aziz U, Adari N, Chaturvedi M, Jules A, Shah I, et al. Self-Administration of Right Vagus Nerve Stimulation Activates Midbrain Dopaminergic Nuclei. Front Neurosci. 2021;15:782786.
68. Peanlikhit T, Van Waes V, Pedron S, Risold P-Y, Haffen E, Etiévant A, et al. The antidepressant-like effect of tDCS in mice: a behavioral and neurobiological characterization. Brain Stimulat. 2017;10:748–56.
69. Chib VS, Yun K, Takahashi H, Shimojo S. Noninvasive remote activation of the ventral midbrain by transcranial direct current stimulation of prefrontal cortex. Transl Psychiatry. 2013;3:e268.
70. De Paolis ML, Paoletti I, Zaccone C, Capone F, D'Amelio M, Krashia P. Transcranial alternating current stimulation (tACS) at gamma frequency: an up-and-coming tool to modify the progression of Alzheimer's disease. Transl Neurodegener. 2024;13:33.
71. D'Amelio M, Di Lazzaro V. Can transcranial magnetic stimulation rescue dopaminergic signalling in Alzheimer's disease? Brain J Neurol. 2023;146:e43–e45.
72. De Paolis ML, Loffredo G, Krashia P, La Barbera L, Nobili A, Cauzzi E, et al. Repetitive prefrontal tDCS activates VTA dopaminergic neurons, resulting in attenuation of Alzheimer's Disease-like deficits in Tg2576 mice. Alzheimers Res Ther. 2025;17:94.

ACKNOWLEDGEMENTS

We thank Dr. Wirz for assistance with animal caring and Dr. Latagliata for assistance with HPLC experiments.

AUTHOR CONTRIBUTIONS

Serena Ficchì: Data curation, Methodology, Investigation, Writing – original draft, Writing – review and editing; Emma Cauzzi: Data curation, Methodology, Investigation, Writing – review and editing; Livia La Barbera: Data curation, Methodology, Investigation, Supervision, Writing – original draft, Writing – review and editing, Funding acquisition; Maria Luisa De Paolis: Data curation, Methodology, Investigation, Writing – review and editing; Gilda Loffredo: Data curation, Methodology, Investigation, Writing – review and editing; Elena Spoleti: Data curation, Methodology, Investigation; Irene Ferrari: Data curation, Methodology, Investigation; Luana Saba: Methodology; Filippo Biamonte: Data curation, Methodology; Annalisa Nobili: Methodology, Supervision, Writing – review and editing; Paraskevi Krashia: Conceptualization, Supervision, Data curation, Methodology Writing – original draft, Writing – review and editing, Funding acquisition; Marcello D'Amelio: Conceptualization, Supervision, Writing – original draft, Writing – review and editing, Funding acquisition.

FUNDING

LLB was supported by an under-40 grant from the Italian Association for Alzheimer's Research [AIRALTZH-AGYR2021] and by the Strategic University Projects – Young Researcher Independence [YRG2021] from the Università Campus Bio-Medico di Roma (Rome, Italy). PK was supported by the Italian Health Ministry [Research Grant: GR-2019-12370446] and by the Alzheimer's Association [AARG-22-922961]. MDA was supported by the Alzheimer's Association [AARG-18-566270; AARG-21-851219], by the Italian Health Ministry [Research Grant: RF-2018-12365527], by the Italian Ministry of Universities and Research [Prot. 2020Z73J5A] and by Fondazione Roma (Rome, Italy).

COMPETING INTERESTS

The authors declare no competing interests.

ADDITIONAL INFORMATION

Supplementary information The online version contains supplementary material available at https://doi.org/10.1038/s41398-025-03588-w.

Correspondence and requests for materials should be addressed to Marcello D'Amelio.

Reprints and permission information is available at http://www.nature.com/reprints

Publisher's note Springer Nature remains neutral with regard to jurisdictional claims in published maps and institutional affiliations.